Cryogenics 50 (2010) 231–238

Contents lists available at ScienceDirect

Cryogenics

journal homepage: www.elsevier.com/locate/cryogenics

A model for exergy analysis and thermodynamic bounds of Stirling refrigerators

A. Razani [a,*], C. Dodson [b], T. Roberts [b]

[a] Department of Mechanical Engineering, MSC01 1150, The University of New Mexico, Albuquerque, NM 87131, USA
[b] Air Force Research Laboratory, Kirtland AFB, NM 87117-5776, USA

ARTICLE INFO

Article history:
Received 5 June 2009
Received in revised form 4 December 2009
Accepted 17 December 2009

Keywords:
Stirling refrigerators
Exergy analysis
Cryocoolers
Thermodynamics
Cycle optimization

ABSTRACT

A thermodynamic model based on exergy flow through a Stirling Refrigerator is developed. Important irreversibilities of the refrigerator due to external heat transfer with the reservoirs, heat leak, flow and heat transfer in regenerator are included in the model. Expansion and compression efficiencies are introduced in the model to account for the losses in these processes. The effect of a control phase shift between the mass flow rate and pressure across regenerator on the performance of the refrigerator is presented. Analytical solutions representing important quantities in the design of Stirling refrigerators such as the load curve, cooling power and efficiency in terms of basic system input parameters are developed. Thermodynamic bounds for the performance of Stirling refrigerators are obtained. Results indicating a compromise between cooling power and efficiency that are dependent on the constraint of the system are presented and discussed.

© 2009 Elsevier Ltd. All rights reserved.

1. Introduction

Finite time thermodynamics and entropy generation minimization are established methods of performance analysis and optimization of power and refrigeration cycles [1–3]. Different thermodynamic models of Stirling refrigerators, simplifying the complexity of cyclic heat and mass transfer in different components, have been subject of several studies [4–9], to just name a few. In this study a model for the exergy flow in Stirling refrigerator with emphasis on exergy analysis of regenerator in terms of its inlet and exit parameters is developed. In this manner, important sources of exergy destruction and dimensionless quantities controlling the cooling capacity and efficiency of the refrigerator are developed. Exergy analysis is a powerful method for the design of pulse tube and Stirling refrigerators [10–14]. Exergy flow and analysis of Stirling refrigerators show how the input exergy provided by the power input to the compressor is destroyed as the working fluid goes through its cyclic motion in the system. In addition, cooling capacity and efficiency are obtained in terms of important dimensionless numbers convenient for quantifying the important losses and performance evaluation of Stirling refrigerator at the system level.

An important goal of this study is to find analytical expressions for the thermodynamic bounds of Stirling refrigerators in terms of the most important global variables influencing the performance of the refrigerator. Therefore, the study can be used to assess the effect that changing a global design parameter of the refrigerator can have on a particular aspect of its performance. Depending on the constraint on the system, the study shows that the efficiency and cooling power of the Stirling refrigerator can be two distinct criteria for the optimization of the refrigerator. Regenerator plays a particularly important role on the thermodynamic bounds of Stirling refrigerators and greatly influences its cooling capacity and efficiency. For the purpose of this study, regenerator is conveniently modeled using two free parameters one representing its exergy flow efficiency and the other its thermal ineffectiveness.

Exergy is a function of both the state of a system and the state of the environment as it measures the departure of the state of the system from the state of the environment. In application to Stirling refrigerators, for each component, considering one channel of heat transfer between the system and a thermal reservoir at the temperature T_R and one channel of inlet and exit mass transfer, the exergy balance can be written as [10,12]

$$\dot{E}_D = (\dot{M}e)_i - (\dot{M}e)_e - \dot{W} + \left(1 - \frac{T_o}{T_R}\right)\dot{Q} \tag{1}$$

where e is the specific exergy carried with mass, $\dot{E}_D$ is the rate of exergy destruction in the component, and $\dot{Q}$ is the rate of heat transfer. For a single-component working fluid, such as helium, in the absence of chemical, kinetic, or potential exergy, the specific exergy can simply be written as

$$e = h - h_o - T_o(s - s_o) \tag{2}$$

where h is the specific enthalpy and s is the specific entropy and subscript "o" denotes the environment. Substituting Eq. (2) into

* Corresponding author. Tel.: +1 505 277 1325; fax: +1 505 277 1571.
E-mail address: razani@unm.edu (A. Razani).

0011-2275/$ - see front matter © 2009 Elsevier Ltd. All rights reserved.
doi:10.1016/j.cryogenics.2009.12.007

Nomenclature

A	area of regenerator
C	flow conductance
CHX	Cold Heat Exchanger
C_p	heat capacity at constant pressure
$\dot{E}_D$	rate of exergy destruction
e	specific exergy
h	specific enthalpy
HHX	Hot Heat Exchanger
$\dot{I}$	rate of irreversibility
K	effective thermal conductivity of regenerator
L	length of regenerator
$\dot{m}$	amplitude of mass flow rate
$\dot{M}$	mass flow rate
Mr	mass flow rate amplitude ratio across regenerator
P	pressure
p	pressure amplitude
Pr	pressure amplitude ratio across regenerator
$\dot{Q}$	rate of heat transfer
s	specific entropy
T	temperature
UA	thermal conductance
$\dot{V}$	average effective void volume of regenerator
$\dot{W}$	power
Y	sine of phase angles

Greeks

θ	phase angle for pressure
η	efficiency
ψ_1	dimensionless number, $\dot{m}_2/\dot{C}p_1$
ψ_2	dimensionless number, $\dot{V}\omega/\dot{C}$
ϕ	phase angle for mass flow rate
λ	regenerator ineffectiveness
ω	angular frequency
γ	specific heat ratio
τ	period of oscillation

Subscripts

a	average, ambient
b	bound
c	cold
co	no load
$cond$	conduction
$comp$	compressor
cn	normalized cold side
$cn1$, $cn2$	normalized cold side, Eqs. (24) and (29)
e	exit, expansion
h	hot heat exchanger
ex	exergetic
i	inlet
j	general inlet or exit of components
l	cold heat exchanger
$leak$	heat leak
n	normalized
o	environment
opt	optimum
p	pressure
r	regenerator
R	reservoir
th	thermal
1	hot side of regenerator, Fig. 1
2	cold side of regenerator, Fig. 1
0, 1, 2, 3, 4	used with sine of phase angles, Appendix A.

Eq. (1) and using the vanishing average mass flow rate over a cycle yields

$$\dot{E}_D = (\dot{M}h)_i - (\dot{M}h)_e - T_o[(\dot{M}s)_i - (\dot{M}s)_e] - \dot{W} + \left(1 - \frac{T_o}{T_R}\right)\dot{Q} \tag{3}$$

Assuming the ideal gas law is valid and thermophysical properties are constant, the specific enthalpy and entropy in the above equation can be written respectively as

$$h = C_p(T - T_o) \tag{4}$$

$$s = C_p \ln(T/T_o) - R\ln(P/P_o) \tag{5}$$

2. Exergy based thermodynamic analysis of Stirling refrigerators

Fig. 1 shows important components of a Stirling refrigerator used for analysis in this study. Exergy comes into the system at the driver side from the compressor and is destroyed as it moves through the system. The product exergy is delivered to the cold reservoir at the temperature T_c. The conservation of energy and the balance of exergy for a system composed of compressor and the Hot Heat Exchanger (HHX) at the temperature T_h can be written respectively as

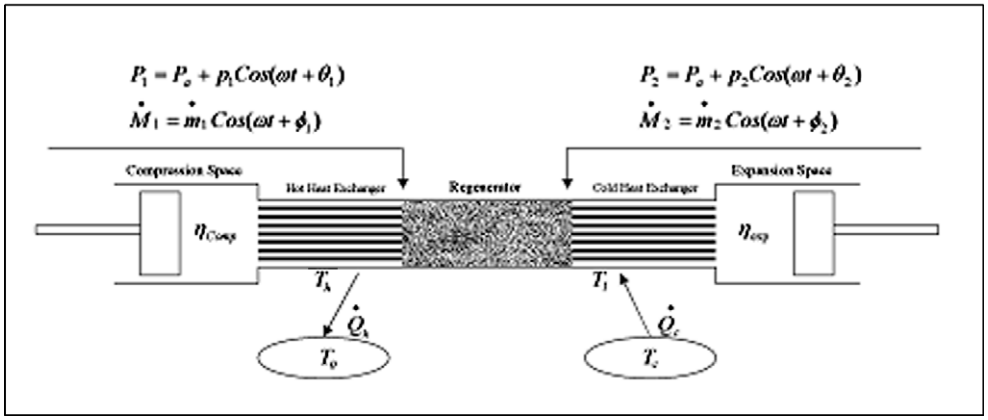

Fig. 1. Schematic of Stirling refrigerator and parameters used in the model.

$$\dot{Q}_h = \dot{W}_{comp} + \dot{W}_e - \dot{Q}_r \tag{6}$$

$$\dot{W}_e + \eta_{comp}\dot{W}_{comp} = \dot{E}_1 + \dot{I}_{HHX} = \dot{E}_1 + \dot{Q}_h\left(1 - \frac{T_o}{T_h}\right) \tag{7}$$

where $\dot{W}_{comp}$ and $\dot{W}_e$ are the input compressor power and power transferred from the expander over a cycle, respectively. $\dot{E}_1$ is the rate of exergy transfer exiting the system, and $\dot{Q}_h$ and $\dot{Q}_r$ are the rate of heat transfer to the hot reservoir and energy transfer to regenerator, respectively. $\dot{I}_{HHX}$ represent the rate of exergy destruction in the HHX and η_{comp} denotes the exergetic efficiency of compressor. We assume for purposes of this study that the mass flow rate and pressure at the inlet and exit of each component are given by

$$\dot{M}_j = \dot{m}_j \cos(\omega t + \phi_j) \tag{8}$$

$$P_j = P_a + p_j \cos(\omega t + \theta_j) \tag{9}$$

Using Eqs. (2), (4), and (5), the pressure component of exergy at any location over a cycle can be written as [12]

$$(\dot{E}_j)_p = \frac{RT_o}{\tau}\int_0^{\tau} \dot{M}_j \ln\left(\frac{P_j}{P_o}\right)dt \tag{10}$$

where τ is the period of oscillation. Using Eqs. (8)–(10) the pressure component of exergy assuming relatively small pressure amplitude ($p_j < 0.3P_a$) can be written as

$$(\dot{E}_j)_p = (1/2)RT_o\dot{m}_j\frac{p_j}{P_a}\cos(\phi_j - \theta_j) \tag{11}$$

The thermal exergy transfer at the cold side of the regenerator due to conduction heat transfer and ineffectiveness of the regenerator can be written as

$$(\dot{E}_2)_{th} = \dot{Q}_r\left(1 - \frac{T_o}{T_l}\right) \tag{12}$$

where T_l is the exit temperature of the regenerator. Using the definition of thermal ineffectiveness of the regenerator, the rate of energy transfer due to the mass flow at the cold side of regenerator can be estimated [12,15]

$$\lambda = \frac{\dot{Q}_2}{(1/\pi)C_p(T_h\dot{m}_1 - T_l\dot{m}_2)} \tag{13}$$

where the denominator represents the maximum rate of enthalpy transfer into the regenerator. Conduction heat transfer to the cold side of regenerator can be estimated assuming a linear temperature profile in the regenerator

$$\dot{Q}_{cond} = (KA/L)(T_h - T_l) \tag{14}$$

where *KA/L* is effective thermal conductance in the regenerator and its shell. It should be pointed out that the direction of the thermal exergy transfer at the cold side of the regenerator is opposite to the direction of heat transfer at the point. Using Eqs. (13) and (14), the rate of heat transfer at the cold side of regenerator can be written as

$$\dot{Q}_r = \dot{Q}_2 + \dot{Q}_{cond} = (1/\pi)\lambda C_p(T_h\dot{m}_1 - T_l\dot{m}_2) + (KA/L)(T_h - T_l) \tag{15}$$

Using Eqs. (11) and (12) the total exergy entering and leaving the regenerator can be written respectively as

$$\dot{E}_1 = (\dot{E}_1)_p + (\dot{E}_1)_{th} = (1/2)RT_o\dot{m}_1\frac{p_1}{P_a}\cos(\phi_1 - \theta_1) + \dot{Q}_r\left(1 - \frac{T_o}{T_h}\right) \tag{16}$$

$$\dot{E}_2 = (\dot{E}_2)_p + (\dot{E}_2)_{th} = (1/2)RT_o\dot{m}_2\frac{p_2}{P_a}\cos(\phi_2 - \theta_2) + \dot{Q}_r\left(1 - \frac{T_o}{T_l}\right) \tag{17}$$

Exergy balance for the Cold Heat Exchanger (CHX) can be written as

$$\dot{Q}_c\left(\frac{T_o}{T_l} - \frac{T_o}{T_c}\right) = \dot{E}_2 - \frac{\dot{W}_e}{\eta_e} + \dot{Q}_{leak}\left(1 - \frac{T_o}{T_l}\right) + \dot{Q}_c\left(1 - \frac{T_o}{T_c}\right) \tag{18}$$

where η_e is the exergetic efficiency of the expander, $\dot{Q}_{leak}$ is heat leak to CHX, and $\dot{Q}_c$ and T_c are the cooling capacity of the refrigerator and the cold reservoir temperature, respectively. The first and last terms of Eq. (18) represent the irreversibility of CHX and the exergy delivered to the cold reservoir, respectively. Using conservation of energy for CHX and expander, Eq. (18) can be used to find the cooling capacity of the refrigerator.

$$\dot{Q}_c = \frac{\eta_e(\dot{E}_2)_p}{\eta_e T_o/T_l - \eta_e + 1} - \dot{Q}_r - \dot{Q}_{leak} \tag{19}$$

The heat transfer analysis of HHX, CHX and the heat leak is simplified using overall heat conductance for the heat exchangers and the heat leak.

$$\dot{Q}_h = UA_h(T_h - T_o) \tag{20}$$

$$\dot{Q}_c = UA_c(T_c - T_l) \tag{21}$$

$$\dot{Q}_{leak} = UA_{leak}(T_a - T_l) \tag{22}$$

where *UA* is the effective thermal conductance and subscripts *h*, *c* and *leak* denote hot, cold and leak, respectively. It is assumed that the heat leak to CHX occurs from a reservoir at the effective temperature of T_a.

It is convenient to define the exergetic efficiency of flow through the regenerator as the ratio of the pressure component of exergy at its cold side to its hot side. Using the definition of the exergetic efficiency of flow through the regenerator Eq. (19) can be written as

$$\dot{Q}_c = \dot{W}_{comp}\frac{\eta_e\eta_r(T_o/T_h + \eta_{comp} - 1)}{1 + \eta_e(T_o/T_l - \eta_r T_o/T_h - 1)} - \dot{Q}_r - \dot{Q}_{leak} \tag{23}$$

where η_r is the exergetic efficiency of flow through the regenerator and can be obtained from the application of Eq. (11) to the inlet and exit of the regenerator. The above equation gives the cooling capacity of Stirling refrigerator in terms of important system parameters and exergetic efficiencies of its major components. For an ideal case were the heat conductance of the cold and hot heat exchangers are infinity, there is no heat leak, the regenerators thermal losses are zero, the efficiencies of the compressor, the expander, and the regenerator are one, Eq. (23) gives the Coefficient of Performance (COP), $\mathrm{COP} = \dot{Q}_c/\dot{W}_{comp} = T_c/(T_o - T_c)$, equal to the Carnot COP. In application of Eq. (23) the relations between important parameters of the system and the quantities $\dot{W}_{comp}$, $\dot{Q}_r$ and η_r must be obtained.

Substituting Eqs. (14), (15), and (22) into Eq. (23) and dividing the results by the quantity $\dot{m}_1 RT_o$ yields

$$\dot{Q}_{cn1} = \frac{\dot{W}_{comp,n}\eta_e\eta_r(T_o/T_h + \eta_{comp} - 1)}{1 + \eta_e(T_o/T_l - \eta_r T_o/T_h - 1)} - \frac{\lambda}{\pi}\frac{\gamma}{\gamma - 1}\left(\frac{T_h}{T_o} - Mr\frac{T_l}{T_o}\right) - \frac{(KA/L)_n(T_h - T_l)}{T_o} - \frac{UA_{leak,n}(T_a - T_l)}{T_o} \tag{24}$$

where $\dot{Q}_{cn1} = \dot{Q}_c/\dot{m}_1 RT_o$, $\dot{W}_{comp,n} = \dot{W}_{comp}/\dot{m}_1 RT_o$, $(KA/L)_n = (KA/L)/\dot{m}_1 R$, $UA_{leak,n} = UA_{leak}/\dot{m}_1 R$, and $Mr = \dot{m}_2/\dot{m}_1$. Therefore, Eq. (24) gives the normalized cooling capacity of the Stirling refrigerator in terms of important global system parameters.

For practical application of the thermodynamic analysis presented in this study, relations between the mass flow, pressure and phase angles at the cold and hot sides of regenerator must be obtained. Oscillating flow of heat and mass transfer in regenerators is very complicated [15]. For thermodynamic analysis we consider a simple model for the regenerator to find the bounds for cooling capacity and efficiency of Stirling refrigerators. The

model considers the most important parameters affecting the regenerator losses including the effect of void in the regenerator. The first order model of the regenerator assumes that the mass flow rate at the cold side of the regenerator can be obtained using a linear relation based on a given appropriately average flow conductance.

$$\dot{m}_2\cos(\omega t+\phi_2)=C\left[p_1\cos(\omega t+\theta_1)-p_2\cos(\omega t+\theta_2)\right] \tag{25}$$

where $\dot{C}$ is properly averaged regenerator flow conductance. In addition, a simple model for the conservation of mass in the regenerator can be written as

$$\dot{m}_1\cos(\omega t+\phi_1)=\dot{m}_2\cos(\omega t+\phi_2)-V\omega[p_1\sin(\omega t+\theta_1)+p_2\sin(\omega t+\theta_2)] \tag{26}$$

where V is the properly averaged effective regenerator void volume including the influence of temperature distribution in the regenerator. Expanding Eqs. (25) and (26), and applying trigonometric identities, results in a set of equations that uniquely determine the relations between the phase shifts and amplitudes of pressure and mass flow rates at the cold and hot sides of the regenerator. These relations are given in Appendix A. Using Eq. (11), the exergetic flow efficiency of regenerator η_r can be written as

$$\eta_r=Mr\,\mathrm{Pr}\frac{\cos(\phi_2-\theta_2)}{\cos(\phi_1-\theta_1)}=Mr\,\mathrm{Pr}\frac{\sqrt{1-Y_0^2}}{\sqrt{1-Y_3^2}} \tag{27}$$

where Pr is the pressure amplitude ratio across the regenerator.

3. Results and discussions

Eq. (24) can be used to calculate the no-load temperature where the left hand side of the equation is zero. Using Eq. (21) this temperature is denoted by T_{co} where $T_l=T_c=T_{co}$. The no-load temperature is of great practical importance in design of cryogenic refrigerators [11]. For the special case of infinite thermal conductance of the HHX, no conduction heat transfer in the regenerator, no heat leak, and no void in the regenerator, Eq. (24) can be considerably simplified and the no-load temperature can be written as solution of a quadratic equation for T_o/T_{co}.

$$\frac{\lambda}{\eta_{comp}\eta_r\pi}\frac{\gamma}{\gamma-1}\left(1-\frac{T_{co}}{T_o}\right)\left(\frac{T_o}{T_{co}}+\frac{1}{\eta_e}-\eta_r-1\right)-\dot{W}_{comp,n}=0 \tag{28}$$

where γ is the specific heat ratio of the working fluid. For a given ratio of pressure amplitude to the system pressure at the inlet of the regenerator, the normalized compressor power is a slowly varying function of the compressor power. Therefore, Eq. (28) shows the secondary effect of the compressor power and the significant influence of the regenerator ineffectiveness on the no-load temperature of Stirling refrigerators. In addition, the equation also shows the effect of exergetic efficiencies of the expander, compressor, and fluid flow through the regenerator on the no-load temperature. It should be pointed out that the reduction in the value of the regenerator ineffectiveness is normally accompanied by a reduction in the exergetic efficiency of the fluid flow in the regenerator. This fact is well-known as an important challenge in the design of regenerators for the Stirling cryogenic refrigerators.

3.1. Analysis for no void in regenerator with zero external irreversibility

Thermodynamic analysis of Stirling refrigerators is considerably simplified when the thermal conductance of the cold and hot heat exchangers are infinity, resulting in zero exergy destruction in the heat exchangers (no external irreversibilities). In addition, if we assume that the conduction heat transfer in the regenerator is zero, there is no heat leak, and no void in the regenerator, Eqs. (17), (19) and A1 can be combined to find the cooling capacity of the refrigerator

$$\dot{Q}_{cn2}=\left[\frac{\eta_e\mathrm{Pr}\cos(\phi_2-\theta_2)}{\eta_eT_o/T_c-\eta_e+1}-\frac{2\lambda}{\pi}\frac{\gamma}{\gamma-1}\frac{P_a}{p_1}\left(1-\frac{T_c}{T_o}\right)\right]\cdot\left[1+\mathrm{Pr}^2-2\mathrm{Pr}\left(\sqrt{\cos^2(\phi_2-\theta_2)(1-\mathrm{Pr}^2\sin^2(\phi_2-\theta_2))}+\mathrm{Pr}\sin^2(\phi_2-\theta_2)\right)\right]^{1/2} \tag{29}$$

where $\dot{Q}_{cn2}=2P_a\dot{Q}/\mathrm{CRT}_op_1^2$. Eq. (29) shows the normalized cooling capacity as a function of the pressure amplitude ratio and the phase shift between the mass flow and pressure at the cold side of the regenerator. The thermodynamic bound of the cooling capacity occurs when the phase shift is zero. In this case Eq. (29) can be considerably simplified and written as

$$\dot{Q}_{cn2,b}=(1-\mathrm{Pr})\left[\frac{\eta_e\mathrm{Pr}}{\eta_eT_o/T_c-\eta_e+1}-\frac{2\lambda}{\pi}\frac{\gamma}{\gamma-1}\frac{P_a}{p_1}\left(1-\frac{T_c}{T_o}\right)\right] \tag{30}$$

In this particular case the pressure amplitude ratio across the regenerator for the maximum cooling capacity can be analytically evaluated.

$$\mathrm{Pr}_{opt}=1/2+\frac{\lambda}{\pi}\frac{\gamma}{\gamma-1}\frac{P_a}{p_1}\left(1-\frac{T_c}{T_o}\right)(T_o/T_c+1/\eta_e-1) \tag{31}$$

For the case of thermally perfect regenerator, when $\mathrm{Pr}_{opt}=1/2$, the thermodynamic bound for the normalized cooling capacity is given by $\dot{Q}_{cn2,b}=\frac{\eta_e}{4(\eta_eT_o/T_c-\eta_e+1)}$. It is interesting to note that from Eqs. (30) and (31) for the Stirling refrigerator to be able to produce any cooling the upper bound of the regenerator ineffectiveness is given by

$$\lambda<\frac{\pi(\gamma-1)}{2\gamma}\frac{p_1}{P_a}\frac{1}{(1-T_c/T_o)(T_o/T_c+1/\eta_e-1)} \tag{32}$$

Eqs. (30) and (31) can be used to find the thermodynamic bound for the no-load temperature for a given λ, p_1/P_a and η_e.

$$(1-T_{co}/T_o)(\eta_eT_o/T_{co}-\eta_e+1)-\frac{\pi(\gamma-1)\eta_ep_1}{2\gamma\lambda P_a}=0 \tag{33}$$

Assuming infinite thermal conductance for the hot and cold heat exchangers and using Eqs. (19) and (23), the expression for the compressor power can be written as

$$\dot{W}_{comp}=\frac{[1+\eta_e(T_o/T_c-\eta_r-1)]\dot{E}_{2p}}{\eta_r\eta_{comp}(\eta_eT_o/T_c-\eta_e+1)} \tag{34}$$

Assuming no heat leak, Eqs. (23) and (34) can be combined to obtain an expression for the Coefficient of Performance (COP) of Stirling refrigerators

$$\mathrm{COP}=\frac{\dot{Q}_c}{\dot{W}_{comp}}=\frac{\eta_e\eta_r\eta_{comp}}{1+\eta_e(T_o/T_c-\eta_r-1)}-\frac{\dot{Q}_r}{\dot{W}_{comp}} \tag{35}$$

Using Eqs. (15) and (34) and assuming no conduction heat transfer in the regenerator, Eq. (35) can be written as

$$\mathrm{COP}=\frac{\eta_e\eta_{comp}\eta_r}{1+\eta_e(T_o/T_c-\eta_r-1)}-\frac{2P_a\eta_r\eta_{comp}\lambda\gamma(\eta_eT_o/T_c-\eta_e+1)(1/Mr-T_c/T_o)}{\pi\,p_1(\gamma-1)[1+\eta_e(T_o/T_c-\eta_r-1)]\mathrm{Pr}\cos(\phi_2-\theta_2)} \tag{36}$$

In Eq. (36) η_r is obtained from Eq. (27) and for the case of no void in the regenerator ($Mr=1$) can be written as

$$\eta_r=\frac{\mathrm{Pr}\cos(\phi_2-\theta_2)}{\sqrt{1-\mathrm{Pr}^2\sin^2(\phi_2-\theta_2)}} \tag{37}$$

Exergetic efficiency can be obtained by dividing the COP by the coefficient of performance of the Carnot cycle, $\eta_{ex} = \mathrm{COP}/\mathrm{COP}_{car} = \mathrm{COP}(T_o/T_c - 1)$. For the case of no void in the regenerator, Eqs. (36) and (37) indicate that the thermodynamic bound for the COP occurs when the mass flow and pressure are in phase at the cold side of regenerator. In this case the optimum COP can be written as

$$\mathrm{COP}_{opt} = \frac{\eta_e \eta_{comp} \mathrm{Pr}}{1 + \eta_e(T_o/T_c - \mathrm{Pr} - 1)} - \frac{2P_a \eta_{comp} \lambda\gamma(\eta_e T_o/T_c - \eta_e + 1)(1 - T_c/T_o)}{\pi\, p_1(\gamma - 1)[1 + \eta_e(T_o/T_c - \mathrm{Pr} - 1)]} \tag{38}$$

The COP corresponding to the optimum cooling capacity can be obtained by substituting Eq. (31) into Eq. (38). For a thermally perfect regenerator, the optimum COP is given by the first term of Eq. (38). Eq. (31) gives $\mathrm{Pr}_{opt} = 1/2$ for a thermally perfect regenerator. In this case the corresponding coefficient of performance at optimum cooling capacity is given by $\mathrm{COP}_{opt} = 1/(2T_o/T_c - 1)$, also reported by de Boer [8]. It is convenient to write Eq. (36) for a given pressure phase shift between the hot and the cold sides of the regenerator. Eqs. (36) and (37) can be combined to find the COP in terms of the pressure phase shift across the regenerator utilizing the following trigonometric equation for the case of no void in the regenerator.

$$\tan(\phi_2 - \theta_2) = \frac{\sin(\theta_1 - \theta_2)}{\cos(\theta_1 - \theta_2) - \mathrm{Pr}} \tag{39}$$

Therefore, for the case of thermally perfect regenerator the COP in terms of the pressure phase shift across the regenerator can be written as

$$\mathrm{COP} = \frac{\eta_e \eta_{comp} \mathrm{Pr}[\cos(\theta_1 - \theta_2) - \mathrm{Pr}]}{1 - \mathrm{Pr}\cos(\theta_1 - \theta_2) + \eta_e\left[\frac{T_o}{T_c}(1 - \mathrm{Pr}\cos(\theta_1 - \theta_2)) + \mathrm{Pr}^2 - 1\right]} \tag{40}$$

The above equation is a convenient analytical expression to find the thermodynamic bound for the COP for a given pressure phase shift across the regenerator and different values of expander and compressor efficiencies. Based on Eq. (40), the thermodynamic bound occurs when the pressure phase shift between the hot and cold side of the regenerator is zero. Therefore, the optimum COP, including the effects of the compressor and expander efficiencies, can be written as

$$\mathrm{COP}_{opt} = \frac{\eta_e \eta_{comp} \mathrm{Pr}(1 - \mathrm{Pr})}{1 - \mathrm{Pr} + \eta_e\left[\frac{T_o}{T_c}(1 - \mathrm{Pr}) + \mathrm{Pr}^2 - 1\right]} \tag{41}$$

In addition, for the ideal case when the compression and expansion efficiencies are one, Eq. (41) gives the coefficient of performance $\mathrm{COP}_{opt} = \mathrm{Pr}/(T_o/T_c - \mathrm{Pr})$, also noted by de Boer [8].

Fig. 2 shows the results of calculations using Eq. (29) for the normalized cooling capacity as a function of the pressure amplitude ratio across the regenerator. The results are given for three values of ineffectiveness and three values of the phase shift between the mass flow and pressure at the cold side of the regenerator. Other values of parameters are given in the figure. It can easily be seen from Eq. (29) that, with the assumptions used to develop the equation, the same cooling capacity is obtained when the phase of mass flow is lagging or leading the pressure phase by the same amount. In addition, the thermodynamic bound for the cooling capacity occurs when the phase shift is zero as discussed previously. The figure shows that the value of the regenerator ineffectiveness has a significant effect on the cooling capacity. In fact, extrapolating the values of the optimum cooling capacity for the zero phase shift, the upper bound for the regenerator ineffectiveness capable of producing any cooling is $\lambda \approx 0.0155$. This value is consistent with the upper bound for the regenerator ineffectiveness given analytically by Eq. (32) for the same parameters used in the figure. Fig. 3 shows the same results as in Fig. 2 for different values of the regenerator ineffectiveness and the expander efficiency. The results are given only when the mass flow and pressure are in phase at the cold side of the regenerator. The optimum values of Pr obtained from the figure correspond to the values obtained analytically from Eq. (31). The results also show the significant effect of the regenerator ineffectiveness on the cooling capacity of the refrigerator while the effect of the expander efficiency is not very significant for the values used in this figure. Fig. 4 shows exergetic efficiency as a function of the pressure amplitude ratio for two values of the regenerator ineffectiveness, different values of the phase shift at the cold side of regenerator, and different values of the pressure phase shift across the regenerator. Other values used in the calculation are reported on the figure. The results are qualitatively different when the phase shift constraint between the mass flow and pressure at the cold side is compared with the pressure phase shift constraint across the regenerator. Exergetic efficiency is a monotonically increasing function of Pr when *Yo* is given while there is an optimum when the *Y1* is the constraint. The calculations in Fig. 4 are based on Eqs. (36), (37), and (39) with Pr as the independent variable. As in Fig. 2, the thermodynamic bound for the exergetic efficiency occurs when the pressure and mass flow are in phase at the cold side

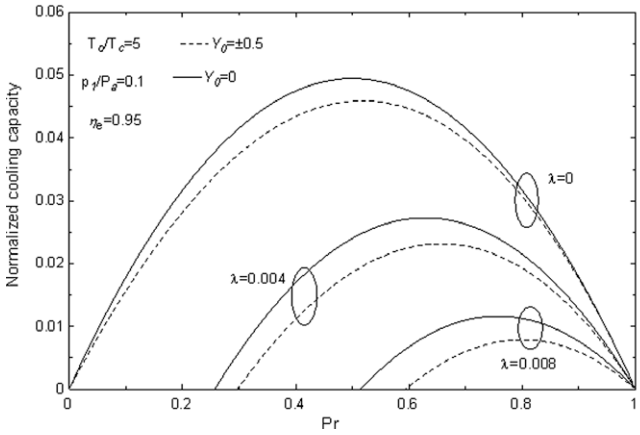

Fig. 2. Normalized cooling capacity as a function of Pr for different values of λ and Y_0.

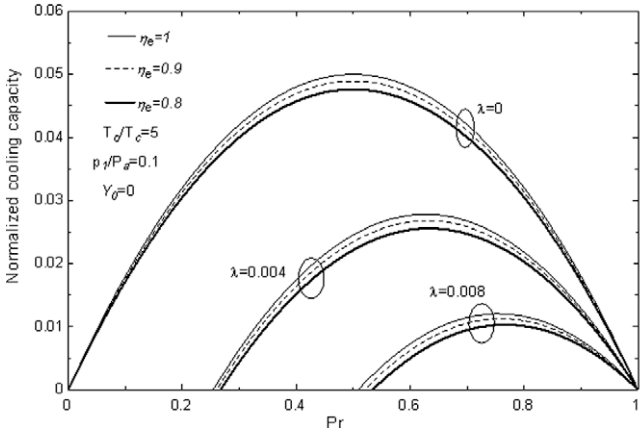

Fig. 3. Normalized cooling capacity as a function of Pr for different values of λ and η_e.

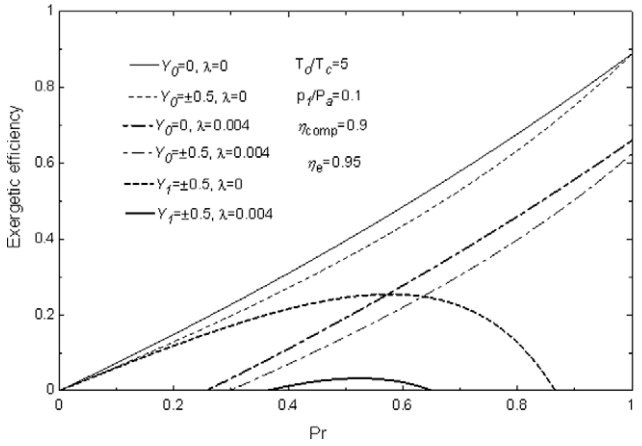

Fig. 4. Exergetic efficiency as a function of Pr for different values of λ and Y_0.

of regenerator. In addition, the efficiency is the same when the mass flow is lagging or leading the pressure by the same amount. Fig. 5 shows the cooling capacity and efficiency diagram for different values of the regenerator ineffectiveness, expansion efficiency, and the phase shift between mass flow and pressure at the cold side of the regenerator. The figure is generated by using Pr as a parameter. The significant influence of the regenerator ineffectiveness is clearly shown in the figure. Fig. 6 shows the cooling capacity and efficiency diagram for different values of the pressure phase shift across the regenerator using Pr as a parameter. Calculations are based on Eqs. (29), (36), (37), and (39). In these calculations the values of Y_1 are fixed and Pr is used as a parameter. The loop-shaped curves in the figure show the compromise between the cooling capacity and efficiency. The values of Pr for the optimum cooling capacity and optimum efficiency are different. As the value of the regenerator ineffectiveness increases the loop-shaped curve becomes smaller, indicating diminished performance of the refrigerator in both cooling capacity and efficiency. In fact, for the case of $Y_1 = \pm 0.2$ and $\lambda = 0.008$ the performance of the refrigerator is drastically reduced for the parameters used in the figure.

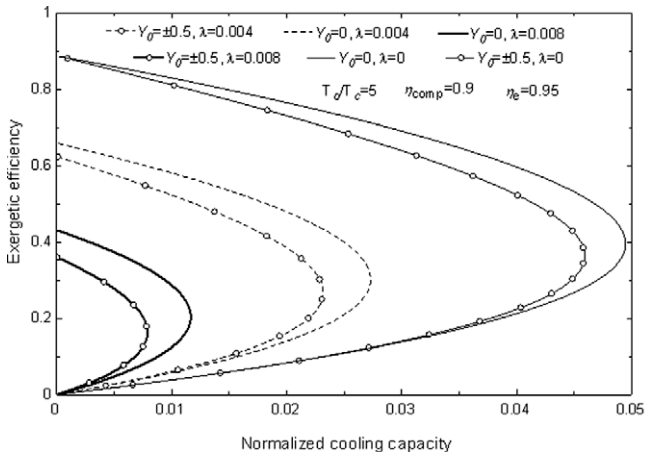

Fig. 5. Normalized cooling capacity and efficiency diagram for different values of λ and Y_0.

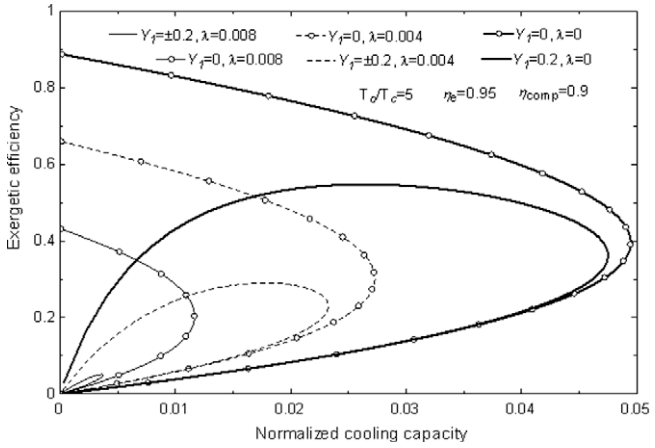

Fig. 6. Normalized cooling capacity and efficiency diagram for different values of λ and Y_1.

3.2. The effect of void in the regenerator and external irreversibilities

The void in the regenerator has important effect on the performance of the Stirling refrigerators. The dimensionless variable representing the void in the regenerator is given by $\psi_2 = V\omega/C$. The relations between the phase shifts at the inlet and exit of the regenerator, including the effect of void, is given in Appendix A. Fig. 7 shows the effect of the void in the regenerator on the normalized cooling capacity and the exergetic efficiency as a function of the pressure amplitude ratio across the regenerator for three values of ψ_2 when the phase shift between the mass flow and pressure at the cold side of the regenerator is zero. The important effect of void in the regenerator is clearly shown. In addition, for one value of the void, $\psi_2 = 0.2$, the figure also gives the results for three values of the phase shift between the mass flow and pressure at the cold side of regenerator. For a given void in the regenerator, the optimum cooling capacity and efficiency are different and are a function of the phase shift. Fig. 8 shows the cooling capacity and efficiency diagram for the same data used in Fig. 7 with Pr as a parameter. With Pr as a parameter, a looped-shape curve can be obtained indicating a compromise between the cooling capacity and efficiency for the cases studied. The optimum efficiency and the optimum cooling capacity are functions of the void in the regenerator and the phase shift as shown it the figure. For a given void in the regenerator, the optimum phase shift can be obtained for the cooling capacity or the efficiency. The figure indicates the potential advantage of actively controlling the phase shift in the Stirling refrigerator to optimize the cooling capacity or efficiency as compared to the passive methods of phase shift control in pulse tube refrigerators.

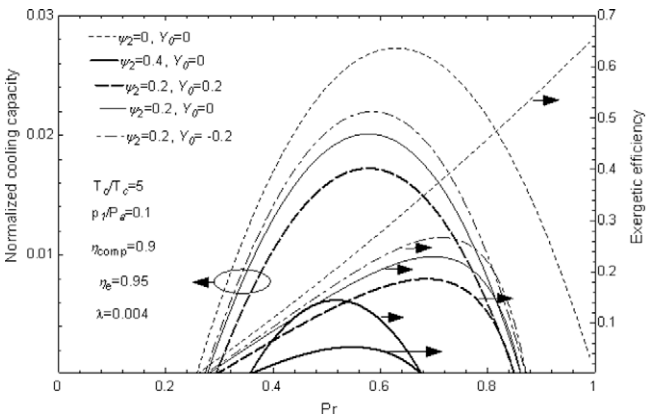

Fig. 7. Normalized cooling capacity and exergetic efficiency as a function of the pressure amplitude ratio across regenerator for different values of ψ_2 and Y_0.

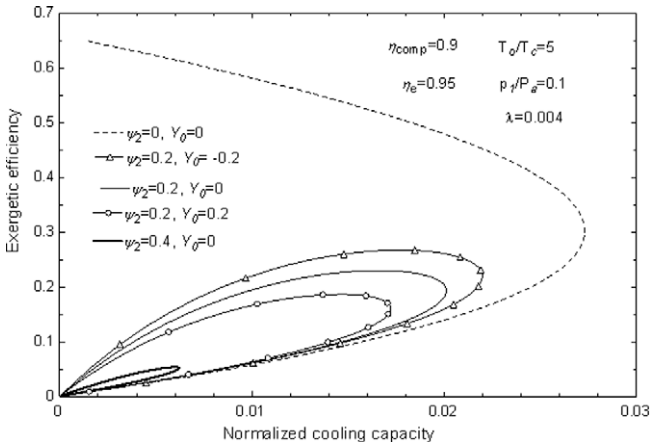

Fig. 8. Normalized cooling capacity and efficiency diagram for different values of ψ_2 and Y_0.

The effect of external irreversibilities due to the finite heat conductance of the heat exchange between the thermal reservoirs and the Stirling refrigerator is given in Fig. 9. In cryogenic refrigerators the magnitude of heat exchange in the hot heat exchanger is much larger than the cold heat exchanger. In this study the normalized thermal conductance of the heat exchangers is defined by $UA_n = 2(UA)P_a/\mathrm{CRT}_o p_1^2$. Fig. 9 shows the cooling capacity and efficiency diagram for three equal values of the normalized thermal conductance for the hot and cold heat exchangers. As expected, the performance of the Stirling refrigerator is reduced when the irreversibility of heat exchange increases. In addition, the figure includes the results for the case when the total heat conductance of the heat exchangers is fixed and the allocation of the thermal conductance to the heat exchangers is varied. The results show the well-known fact that an optimum exists for the allocation of the thermal conductance to the cold and the hot heat exchangers.

3.3. Comparison with the Stirling cryocooler data

In order to directly compare the experimental results for a particular Stirling cryocooler to the control thermodynamic model used in this study, the global control parameters for the cryocooler must be known. Usually Stirling cryocoolers are designed for a specified set point and may not perform as well in off-design conditions; furthermore, global control parameters are not reported. The most important data usually reported for Stirling type cryocoolers are the load curves ($\dot{Q}_c$ vs. T_c) for different ambient temperatures and the compressor power. The no-load temperature and the coefficient of performance are also usually reported. As an example, the performance data for the CryoTel™ Stirling cryocooler developed by Sunpower are selected to show that the results from the characterization of the cryocooler correspond to the results obtained in this study [16,17]. One of the characteristics of the load curves for Stirling type cryocooler is the near linear variation of load curves for a given compressor power. This can be easily seen from Eq. (36) where for a given compressor power the variation of $\dot{Q}_c$ is a nearly linear function of T_c. In addition, for a given ambient temperature, the no-load temperature is a slowly varying function of the compressor power. This behavior can be seen from Eq. (28) where the combined effect of the thermodynamic parameters is a slowly varying function of the compressor power. For example, for the CryoTel CT Stirling cryocooler, a compressor power of 40 W produces a no-load temperature of approximately 52 K while a compressor power of 160 W results in a no-load temperature of approximately 32 K [16]. This characteristic of the load curves is shown in the performance curves of many Stirling type cryocoolers characterized in our laboratory [11]. The effect of ambient temperature on the performance of Stirling cryocooler can be easily seen in analytical expressions developed in this study because *To* is a control parameter in the model and is also used as a parameter for characterization of Stirling crycoolers. A recent single stage Sunpower Stirling cryocooler (CryoTel LT) can produce a very low no-load temperature of about 21.5 K for the ambient temperature of 310 K [17]. It is interesting to compare this temperature to the thermodynamic bound developed in this study given by Eq. (33). As can be seen from the equation, this is only possible by designing a regenerator for the cryocooler with a very low value of thermal ineffectiveness. The regenerator for the CryoTel LT single stage Stirling cryocooler is carefully designed to produce such a low no-load temperature [17]. Eq. (36) clearly shows the important influence of compressor efficiency and the regenerator exergetic flow efficiency along with its ineffectiveness on the efficiency of the Stirling refrigerator. Well-designed Stirling cryocoolers currently reach the exergetic efficiency of 25% [16,17]. Recently, the increase in compressor efficiency is expected to result in the development of a Stirling cryocooler with exergetic efficiency of close to 30% [18]. It should be pointed out that, as shown in this study, exergetic efficiency and cooling capacity can be two different optimization criteria in the design of Stirling crycoolers.

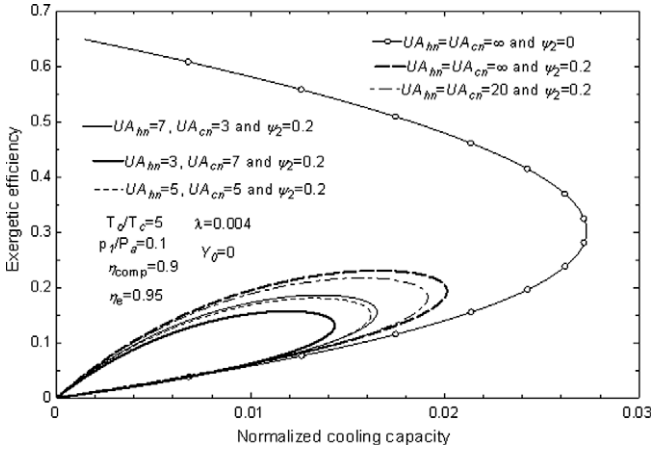

Fig. 9. Normalized cooling capacity and efficiency diagram for different values of UA_{hn} and UA_{cn}.

4. Conclusions

A thermodynamic model based on exergy flow for application to Stirling refrigerators is developed. The model includes the important sources of exergy destruction in the refrigerator. For the case of no void in the regenerator and no exergy destruction in the hot and cold heat exchangers, analytical solutions and thermodynamic bounds for the performance of the refrigerator are obtained. The pressure ratio across the regenerator plays an important role in the development of the analytical solutions in this study. It is shown the under particular constraints one can obtain a loop-shaped curve for the cooling capacity and efficiency diagram, indicating a compromise between the cooling capacity and efficiency. The significant influence of the regenerator effectiveness and the void in the regenerator on the refrigerator performance is noted. An exergetic efficiency parameter defined for the fluid flow in the regenerator facilitates the thermodynamic analysis of the Stirling refrigerator and the development of thermodynamic bounds for the refrigerator. The effect of the size of hot and cold heat exchangers, represented by their values of thermal conductance on the performance of the Stirling refrigerator, is eval-

uated. In this study we have formulated the results in terms of non-dimensionalized variables which are convenient for optimization, parametric studies and obtaining the thermodynamic bounds of the Stirling refrigerators.

Appendix A

Important phase angles for the pressure and mass flow rate across regenerator in terms of dimensionless parameters are given below. These equations are the results of the trigonometric identities applied to Eqs. (25) and (26). Therefore, all trigonometric functions used in Eqs. (25) and (26) can be uniquely determined.

$$\psi_1 = \left[1 + \mathrm{Pr}^2 - 2\mathrm{Pr}\left(\sqrt{(1-Y_0^2)(1-\mathrm{Pr}^2Y_0^2)} + \mathrm{Pr}Y_0^2\right)\right]^{1/2} \tag{A1}$$

$$Y_1 = Y_0\left[\sqrt{1-\mathrm{Pr}^2Y_0^2} - \mathrm{Pr}\sqrt{1-Y_0^2}\right] \tag{A2}$$

$$Mr^2 + 1 - 2Mr\left[\sqrt{(1-Y_2^2)(1-Y_0^2)} + Y_0Y_2\right] - (Mr\psi_2/\psi_1)^2\left(1 + \mathrm{Pr}^2 + 2\mathrm{Pr}\sqrt{1-Y_1^2}\right) = 0 \tag{A3}$$

$$\sqrt{(1-Y_2^2)(1-Y_1^2)} + Y_1Y_2 - Mr\left[\sqrt{(1-Y_0^2)(1-Y_1^2)} + Y_0Y_1\right] + \mathrm{Pr}\sqrt{1-Y_2^2} - Mr\mathrm{Pr}\sqrt{1-Y_0^2} = 0 \tag{A4}$$

$$Y_3 = Y_2\sqrt{1-Y_1^2} - Y_1\sqrt{1-Y_2^2} \tag{A5}$$

where the dimensionless parameters $\psi_1 = \dot{m}_2/Cp_1$ and $\psi_2 = V\omega/C$ are defined representing the physical and thermal properties of the regenerator. Therefore, using the above five equations, for selected parameters such as $Y_0 = \sin(\phi_2 - \theta_2)$, Pr, and ψ_2, the parameters ψ_1, Mr, $Y_1 = \sin(\theta_1 - \theta_2)$, $Y_2 = \sin(\phi_1 - \theta_2)$, $Y_3 = \sin(\phi_1 - \theta_1)$, and $Y_4 = \sin(\phi_1 - \phi_2)$ can be obtained.

References

[1] Berry RS, Kazakov VA, Sieniutycz S, Szwast Z, Tsirlin AM. Thermodynamic optimization of finite time processes. New York: John Wiley and Sons, LTD.; 2001.
[2] Salamon P, Nulton JD, Siragusa G, Andersen TR, Limon A. Principles of control thermodynamics. Energy 2001;26:307–19.
[3] Bejan A. Entropy generation minimization: the method of thermodynamic optimization of finite-size systems and finite time processes. Boca Raton: CRC Press, Inc.; 1996.
[4] Chen J. Minimum power input of irreversible stirling refrigerator for given cooling rate. Energy Convers Manage 1998;39:1255–63.
[5] Chen J, Yan Z. The general performance characteristics of a Stirling refrigerator with regenerative losses. J Phys D: Appl Phys 1996;29:987–90.
[6] Tyagi SK, Kaushik SC, Singhal MK. Parametric study of irreversible Stirling and Ericsson cryogenic refrigeration cycles. Energy Convers Manage 2002;43:2297–309.
[7] Erbay B, Yavuz H. The maximum cooling density of a realistic Stirling refrigerator. J Phys D: Appl Phys 1998;31:291–3.
[8] de Boer PCT. Maximum attainable performance of Stirling engines and refrigerators. J Heat Transfer 2003;125:911–5.
[9] de Boer PCT. Basic limitations on the performance of Stirling cryocoolers. Adv Cryogen Eng 2004;49(B):1396–403.
[10] Razani A, Flake B, Yarbrough S. Exergy flow in Orifice Pulse tube refrigerators and their performance evaluation based on exergy analysis. Adv Cryogen Eng 2004;49(B):1508–18.
[11] Razani A, Flake B, Yarbrough S, Abhyankar NS. Power efficiency diagram for performance evaluation of cryocoolers. Adv Cryogen Eng 2004;49(1):1527–35.
[12] Razani A, Roberts T, Flake B. A thermodynamic model based on exergy flow for analysis and optimization of pulse tube refrigerators. Cryogenics 2007;47:166–73.
[13] Kirconnell CS, Price KD. Thermodynamic optimization of multistage cryocoolers. Cryoccolers 2001;11:69–78.
[14] Kittle P. Enthalpy, entropy, and exergy flows- real gas effects in ideal pulse tube cryocoolers. Adv Cryogen Eng 2006;51(A):345–52.
[15] Ackermann AR. Cryogenic regenerative heat exchangers. New York: Plenum Press; 1997.
[16] Unger R, Keitle D. The development of the CryoTel™ family of coolers. Adv Cryogen Eng 2004;49(B):1404–10.
[17] Unger R. The development of the CryoTel™ LT and GT family. Adv Cryogen Eng 2006;51(1):1719–25.
[18] Willems D, Mullie J, Van de Groep W, Benschop T. Increased capacity cryocoolers at Thales cryogenics BV. Adv Cryogen Eng 55(B), in press.